Neuroimage: Reports 2 (2022) 100134

Contents lists available at ScienceDirect

Neuroimage: Reports

journal homepage: www.sciencedirect.com/journal/neuroimage-reports

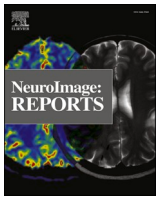

fMRI BOLD and MEG theta power reflect complementary aspects of activity during lexicosemantic decision in adolescents with ASD

M. Wilkinson [a,b], R.J. Jao Keehn [b], A.C. Linke [b], Y. You [c], Y. Gao [a,b], K. Alemu [b], A. Correas [c], B.Q. Rosen [c], J.S. Kohli [a,b], L. Wagner [c], A. Sridhar [b], K. Marinkovic [a,c,d], R.-A. Müller [a,b,*]

[a] San Diego State University/University of California San Diego Joint Doctoral Program in Clinical Psychology, San Diego, CA, United States
[b] Brain Development Imaging Laboratories, Department of Psychology, San Diego State University, San Diego, CA, United States
[c] Spatiotemporal Brain Imaging Laboratory, Department of Psychology, San Diego State University, San Diego, CA, United States
[d] Radiology Department, University of California at San Diego, CA, United States

ARTICLE INFO

Keywords:
Functional magnetic resonance imaging (fMRI)
Magnetoencephalography (MEG)
Multimodal integration
Autism spectrum disorder (ASD)
Lexicosemantic processing
Executive function

ABSTRACT

Neuroimaging studies of autism spectrum disorder (ASD) have been predominantly unimodal. While many fMRI studies have reported atypical activity patterns for diverse tasks, the MEG literature in ASD remains comparatively small. Our group recently reported atypically increased event-related theta power in individuals with ASD during lexicosemantic processing. The current multimodal study examined the relationship between fMRI BOLD signal and anatomically-constrained MEG (aMEG) theta power. Thirty-three adolescents with ASD and 23 typically developing (TD) peers took part in both fMRI and MEG scans, during which they distinguished between standard words (SW), animal words (AW), and pseudowords (PW). Regions-of-interest (ROIs) were derived based on task effects detected in BOLD signal and aMEG theta power. BOLD signal and theta power were extracted for each ROI and word condition. Compared to TD participants, increased theta power in the ASD group was found across several time windows and regions including left fusiform and inferior frontal, as well as right angular and anterior cingulate gyri, whereas BOLD signal was significantly increased in the ASD group only in right anterior cingulate gyrus. No significant correlations were observed between BOLD signal and theta power. Findings suggest that the common interpretation of increases in BOLD signal and theta power as 'activation' require careful differentiation, as these reflect largely distinct aspects of regional brain activity. Some group differences in dynamic neural processing detected with aMEG that are likely relevant for lexical processing may be obscured by the hemodynamic signal source and low temporal resolution of fMRI.

1. Introduction

Autism spectrum disorder (ASD) is a neurodevelopmental disorder characterized by socio-communicative impairments and restricted, repetitive behaviors (American Psychiatric Association, 2013). Many individuals with ASD show delays, impairment, or complete lack of language (Boucher, 2003). A language domain often impacted in ASD is lexicosemantic processing (Bavin et al., 2016; Boucher, 2012; Groen et al., 2008; Kamio et al., 2007; McGregor et al., 2012; Naigles and Tek, 2017). Some previous functional magnetic resonance imaging (fMRI) studies examining lexicosemantic processing reported greater temporo-occipital activation but reduced frontal activity in ASD compared to typically developing (TD) groups (Gaffrey et al., 2007; Harris et al., 2006; Just et al., 2004; Knaus et al., 2017; Lo et al., 2013).

fMRI detects neural activity through changes in blood oxygenation at good spatial, but low temporal, resolution (due primarily to a lag in the hemodynamic response), which has resulted in a predominant neglect of brain dynamics in the fMRI literature and a movement toward multimodal integration (Bolton et al., 2020; Liu et al., 2015; Mash et al., 2018; Padmanabhan et al., 2017). Multimodal studies capturing both temporal dynamics and spatial localization are indispensable for comprehensive models of cognitive and language processing. Some studies attempting to link localized task-related neural activity detected with fMRI with measures derived from neuroimaging modalities with high temporal resolution, such as electroencephalography (EEG) and magnetoencephalography (MEG), have yielded strong associations (including both positive and negative correlations; Ekstrom et al., 2009; Meltzer et al., 2007; Scheeringa et al., 2009; Scheeringa and Fries, 2019; Winterer

* Corresponding author. San Diego State University, 6363 Alvarado Ct., Suite 103, San Diego, CA 92120, United States.
E-mail address: rmueller@sdsu.edu (R.-A. Müller).

https://doi.org/10.1016/j.ynirp.2022.100134
Received 24 March 2022; Received in revised form 4 August 2022; Accepted 5 September 2022

et al., 2007). Methods that detect postsynaptic currents, such as EEG and MEG, have exquisite temporal resolution suitable for the study of brain dynamics. Event-related theta power (4–7 Hz) detected with these techniques is considered the standard for detecting neural activity changes related to cognitive control, working memory, and language processing (Audrain et al., 2020; Bakker-Marshall et al., 2018; Bastiaansen et al., 2005; Begus and Bonawitz, 2020; Halgren et al., 2015; Kovacevic et al., 2012; Marinkovic et al., 2012, 2019; Pu et al., 2020), as well as the transfer of information between brain regions (Begus and Bonawitz, 2020; Marinkovic et al., 2019).

Studies relating BOLD signal to theta power have remained primarily limited to neurotypical adults and the use of EEG (rather than MEG). One resting-state EEG study in children revealed decreased theta power in ASD compared to TD children, which was associated with greater ASD symptomatology (Hornung et al., 2019). Another EEG study reported that a neurotypical increase in theta power associated with increasing working memory load was absent in adults with ASD (Larrain-Valenzuela et al., 2017), and furthermore, that this lack of theta power increase was associated with greater ASD symptomatology. Research using MEG to examine theta power in ASD has been minimal. In one of the few MEG studies on lexicosemantic processing in ASD, members of our group recently reported atypically increased event-related theta power in adolescents with ASD in multiple fronto-temporal brain regions (You et al., 2020). This appears to be in partial contrast to BOLD fMRI findings of atypically *reduced* frontal activity in ASD (Gaffrey et al., 2007; Harris et al., 2006; Just et al., 2004; Knaus et al., 2017), which raises the question whether MEG and fMRI, when implemented in isolation (as has been standard practice), can provide comprehensive assays of neurofunctional differences between ASD and TD samples.

Following up on our unimodal (anatomically-constrained MEG [aMEG]) report (You et al., 2020), the current study, which included an expanded, but partially overlapping sample, investigated the relation between BOLD signal and event-related theta power during lexicosemantic decision in two sets of regions that were (1) reported to show aMEG activity by You et al. (2020), and (2) identified based on increases in task-driven fMRI BOLD signal.

2. Methods

2.1. Participants

Thirty-three ASD and 23 TD participants (aged 12–21 years) were selected from an initially screened sample of 156 ASD and 120 TD adolescents (see supplement for details on exclusions and data loss). ASD diagnoses were based on DSM-5 criteria (American Psychiatric Association, 2013), the Autism Diagnostic Observation Schedule, 2nd Edition (ADOS-2; Lord et al., 2012), and the Autism Diagnostic Interview-Revised (ADI-R; Rutter et al., 2003), as well as expert clinical judgment. Twelve ASD participants were currently taking psychotropic medications (Supplemental Table S1). Fourteen ASD individuals reported comorbidities: 4 with attention-deficit/hyperactivity, 7 with anxiety, and 4 with depression; 2 of these adolescents reported multiple comorbidities (Supplemental Table S1). Presence of comorbidities and use of psychotropic medications were not considered exclusionary as they are common in adolescents with ASD and their exclusion would have rendered the sample less representative of the broader ASD population (Gurney et al., 2006). There was some overlap between this study and You et al. (2020). Fourteen ASD and 16 TD participants were included in both You et al. (2020) and the current study. Five ASD and 4 TD participants were included in You et al. (2020), but not in the current study. Nineteen ASD and 7 TD participants were new to the current study. Informed assent and consent were obtained from all participants and their parents/guardians in accordance with the San Diego State University (SDSU) and the University of California San Diego (UCSD) Institutional Review Boards. Groups did not differ on age, gender, IQ, or handedness (Table 1). As expected, groups differed on task accuracy. Only participants with usable data in *both* fMRI and aMEG modalities were included in analyses.

2.2. Experimental design

Participants completed the Word Reading subtest of the Wechsler Individual Achievement Test, 3rd Edition (WIAT-III; Wechsler, 2009) to assess reading level. Those who received a standard score below 80, which is the average based on 12-year-old reading norms (i.e., a 6th grade reading level), were excluded. Participants were administered the Edinburgh Handedness Inventory (Oldfield, 1971), the Wechsler Abbreviated Scale of Intelligence, 2nd Edition (WASI-II; Wechsler, 2011), the Beery-Buktenica Developmental Test of Visual-Motor Integration, 6th Edition (Beery VMI-6; Beery et al., 2010), and the Clinical Evaluation of Language Fundamentals, 5th Edition (CELF-5; Semel et al., 2013). MEG and MRI scans were completed in subsequent sessions with a counterbalanced order of scans. MEG and MRI data were collected within 150 days of one another, except for 2 ASD participants (174 and 184 days) and 1 TD participant (252 days). To address any potential sensory sensitivities and overall anxiety, participants underwent a mock

Table 1
Participant demographics.

	ASD (n = 33)		TD (n = 23)			χ2 (df)	p
Gender	24 male, 9 female		18 male, 5 female			.22 (1)	.64
Handedness	31 right, 1 left, 1 ambidextrous		21 right, 2 left			1.52 (2)	.47
	Mean (SD)	**Range**	**Mean (SD)**	**Range**	**Cohen's d**	***t*-stat (df)**	***p***
Age (years)	15.77 (2.30)	12.25–20	15.28 (1.93)	12.33–21.42	.23	1.02 (54)	.31
MRI Task Accuracy (%)	88 (8)	71–99	94 (3)	85–99	−.93	3.70 (47.08)	.0006***
MEG Task Accuracy (%)	87 (8)	68–99	92 (6)	70–98	−.69	2.08 (54)	.04*
MRI RMSD	.07 (.03)	.03–.14	.06 (.02)	.03–.13	.38	2.24 (54)	.03*
WASI-II							
Full Scale IQ	107.64 (17.86)	59–136	112.35 (12.94)	88–135	−.29	1.08 (54)	.28
Verbal IQ	105.33 (16.51)	68–134	111.26 (13.08)	85–135	−.39	1.43 (54)	.16
Non-Verbal IQ	109.97 (21.70)	54–156	110.30 (12.31)	80–128	−.02	.07 (52.19)	.94
ADOS-2							
Total	11.06 (3.37)	6–20	–	–	–	–	–

Note: Means, standard deviations (SD), and ranges for each group. Chi-square tests (gender, handedness) and *t*-tests were performed to determine if groups were significantly different on demographic variables. Non-standard degrees of freedom are attributed to Levene's test for homogeneity of variance, and thus reject the null hypothesis of equal variance. * denotes $p \leq .05$, ** $p \leq .01$, *** $p \leq .001$.
ASD = autism spectrum disorder.
RMSD = root mean square difference.
TD = typically developing.

scan prior to the actual MRI scan to familiarize themselves with the environment. During the mock and MRI scans participants were given ear plugs to reduce noise, had cushions surrounding their ears and under their legs for sound reduction and comfort, and were offered a blanket for warmth. MRI operators were in frequent contact with participants throughout the scan and assessed the participants' wellbeing. Similar steps were taken to ensure comfort during the MEG scan. Refer to supplement for additional scan environment information.

During the task, participants were asked to respond differentially to three conditions: real non-animal standard words (SW), animal words (AW), and pseudowords (PW). The task was adapted from an aMEG study in neurotypical adults by Marinkovic and colleagues (2012; 2014). PW trials were designed to be orthographically and phonologically legal letter strings with no meaning (e.g., "blont"). Participants used their left hand to respond on a 2-button fORP 904 response pad (Cambridge Research Systems Ltd., Rochester, UK, https://www.crsltd.com), and were instructed to press the button under their index finger for SW, the button under their middle finger for AW, and to withhold pressing any button for PW. Conditions did not significantly differ on word length or number of syllables; SW and AW conditions did not differ on the frequency of occurrence based on the Zipf scale (Brysbaert and New, 2009; Van Heuven et al., 2014) or age of acquisition (Supplemental Table S2; Kuperman et al., 2012). A practice test was administered while participants lay supine in a mock MRI scanner to simulate the actual MRI scan. Words used during practice differed from those presented during the fMRI and MEG scans.

In the fMRI task, each word was visually presented for 500 ms, followed by a fixation string ("xxxxxx") for 1500 ms (given insertion of additional null trials in fMRI, see below). For the MEG trials, stimuli were also presented for 500 ms in a randomized order, followed by a fixation string for 2000 ms, with no jitter. Stimuli were presented using Presentation® software (Version 22.1, Neurobehavioral Systems, Inc., Berkeley, CA, www.neurobs.com) in white lower-case letters on a black background. Trials were presented in the same order to all participants except 2 ASD and 2 TD adolescents who were scanned a second time due to technical issues and were presented with a different sequence to avoid practice effects. Different stimulus sets were used during MEG and fMRI scans. During MEG scans, task stimuli were presented in a randomized order during an approximately 25-min run, with short breaks every 4 min; 100 words were presented and analyzed for each word condition. An additional 180 SW words were presented as fillers to establish a prepotent response tendency. For fMRI scans, the task was split into two 7-min runs with a 3-min break between runs. Each fMRI run consisted of 90 SW trials, and 30 trials each for AW and PW conditions.

2.3. Experimental stimulus trial structure

RSFgen, a random stimulus function generator in Analysis of Functional NeuroImages (AFNI; Cox, 1996; https://afni.nimh.nih.gov), was used to create the trial sequence in the event-related design. During null trials (in fMRI only), a fixation string ("xxxxxx") was shown. There were 124 1-s null trials ("xxxxxx") per run. Refer to supplement for additional information.

2.4. MEG acquisition and processing

MEG scans were acquired at the UCSD Radiology Imaging Laboratory. Data were acquired from 204 planar gradiometers (102 pairs) using a whole-head Neuromag Vectorview system (Elekta AB, Stockholm, Sweden). To co-register MEG with structural MRI scans, a 3Space Isotrak II (Polhemus Inc., Colchester, VT) was used to digitize fiduciary points (nasion and periauricular points), head position indicator coils, and many other random points on the scalp. A 1000 Hz sampling rate and minimal filtering (0.1–300 Hz) were used to record signals continuously. Matlab scripts (Mathworks Inc., Natick, MA, USA), utilizing Fieldtrip (Oostenveld et al., 2011), EEGLab (Delorme and Makeig, 2004), and MNE (Gramfort et al., 2014), were used for processing and analyzing MEG data as previously described (Beaton et al., 2018; Correas et al., 2019; Kovacevic et al., 2012; Marinkovic et al., 2012, 2019; Rosen et al., 2016). Data were downsampled to 250 Hz, bandpass filtered (0.1–100 HZ), epoched from −300 to 1100 ms for stimulus-locked analysis, and baseline-corrected using the prestimulus period (−300 to 0 ms). Artifacts, such as eyeblinks and heartbeat, were removed using ICA (Delorme and Makeig, 2004), with additional artifacts identified by visual inspection and removed using threshold rejection (Oostenveld et al., 2011). Analyses were conducted on artifact-free trials with correct task response.

Complex wavelet power spectra were calculated across all epochs by convolving them with Morlet wavelets (Lachaux et al., 1999) for the theta band (4–7 Hz, in 1 Hz increments), with a frequency resolution of 2 Hz and time resolution of 80 ms. To remove edge artifacts, padding of 300 ms was added to the two ends of each epoch and subsequently removed after wavelet analysis. Source power estimates were calculated with an aMEG approach (Dale et al., 2000; Marinkovic, 2004), by applying cortically constrained minimum norm estimation to the complex wavelet power spectrum (Kovacevic et al., 2012; Marinkovic et al., 2012, 2019). Noise covariance matrix was estimated by pooling empty room data across sessions, which were band-pass filtered (3–50 Hz). For each participant, total theta source power was estimated at each location on the cortical surface, averaging across theta frequency (4–7 Hz) and artifact-free, correct trials for each condition. Finally, event-related theta power estimates were calculated as percent signal change from the prestimulus baseline (−300 to 0 ms). Structural MRI scans obtained for all participants were analyzed with Freesurfer (Dale et al., 1999; Fischl et al., 1999a). Each participant's reconstructed cortical surface served to constrain inverse solutions (Dale et al., 2000; Marinkovic et al., 2003). Inner skull surface derived from segmented MRI data was used for a boundary element model of the volume conductor. To conduct the group analysis, the reconstructed individual surfaces were morphed into an average representation by aligning their sulcal-gyral patterns (Fischl et al., 1999b) and decimated, defining the solution space with 5124 free-rotating dipoles spaced ~7 mm apart. Group average maps were then computed by averaging individual source power estimates for each group and word condition.

2.5. MRI acquisition and processing

MRI scans were acquired at the UCSD Center for fMRI with a General Electric Discovery MR750 3.0 T scanner (GE Healthcare, Milwaukee, WI) and a Nova Medical 32-channel head coil. Structural scans were acquired using a Fast Spoiled Gradient Recalled T1-weighted sequence (TR: 8.136 ms; TE: 3.172 ms; flip angle: 8°; FOV: 25.6 cm; acquisition matrix: 256x256; slices: 172; voxel size: 1 mm^3; duration: 5min). Functional scans were acquired using a multi-echo simultaneous multislice (MESMS) T2*-weighted echo planar imaging (EPI) sequence (volumes: 340; TR:1250 ms; TEs: 13.2, 30.3, 47.4 ms; flip angle: 60°; FOV: 21.6 cm; acquisition matrix: 72x36; acceleration factor [R]: 2; slices: 54; voxel size: 3 mm^3). Data from ten participants (9 TD, 1 ASD) were collected using a slightly different protocol due to a technical error at early stages of the study (all parameters identical except volumes: 386; TR: 1100; slices: 45). The first 9 volumes were discarded to allow for magnetization to reach equilibrium. The MESMS protocol includes simultaneous acquisition of multiple slices at multiple echo times, with increased signal-to-noise ratio (Kundu et al., 2012, 2013; Olafsson et al., 2015).

fMRI data were preprocessed and analyzed using AFNI (Version 19.0.00), FSL (Version 5.0), and Matlab (2013b). Echo-planar images (EPI) for each echo time were corrected for susceptibility-induced distortions with FSL's TOPUP tool, using two spin-echo acquisitions with opposite phase encoding directions (Smith et al., 2004). Rigid-body realignment of each functional volume to the middle volume was performed using AFNI and head motion quantified as the root mean square

difference (RMSD) from the six motion parameters of the 30.3 ms echo time data. EPIs from the three echoes were optimally combined (Kundu et al., 2013). Data were denoised with multi-echo ICA (ME-ICA; Olafsson et al., 2015) using meica.py (openly available on Github, https://github.com/ME-ICA/me-ica). ME-ICA has been shown to be superior to standard denoising processes (Lynch et al., 2020), allowing for removal of artifacts (non-BOLD components) from the BOLD signal (Kundu et al., 2013). FSL FLIRT was used to co-register functional and structural scans, and FNIRT to reorient images to MNI-152 space. Data were spatially smoothed using a Gaussian kernel of 6 mm FWHM in AFNI's 3dBlurToFWHM and scaled to percent signal change. Functional data of the two runs were concatenated for each participant and analyzed in AFNI using 3dBandPass for temporal filtering ($f > .008$ Hz).

2.6. General linear model

3dDeconvolve was used to perform an ordinary least squares (OLS) regression on the functional data. Regressors included the three word conditions of interest (SW, AW, and PW). A two-parameter statistical parametric mapping (SPM) gamma variate basis function approximated the canonical hemodynamic response function. 3dREMLfit was used to conduct a residual maximum likelihood estimation, which takes into consideration the residuals of the time series and uses an autoregressive moving average (ARMA[1,1]) model, for each participant on a voxel-wise basis through a generalized least squares time series fit. The estimates of effect size (beta coefficients) were output and used for subsequent group comparisons.

2.7. ROI identification

FMRI-derived and MEG-derived ROIs were two separate sets in largely different brain regions. Regions of activation were identified from MEG scans that were based on cortical surfaces reconstructed with FreeSurfer, serving to constrain inverse estimates. These MEG-derived ROIs were then transformed into volumetric space to be used with fMRI data. Regions of activation were also identified from fMRI scans, and these fMRI-derived ROIs were then transformed into surface space for use with MEG data. Refer to the aMEG and fMRI sections below, as well as the supplement, for further details on ROI identification and transformation.

2.7.1. aMEG

aMEG-derived ROIs were adopted from You et al. (2020) and consisted of regions with significant source power based on an average of all participants and word conditions. aMEG-derived ROIs were transformed into volumetric space using FreeSurfer (Dale et al., 1999) to test if prominent group differences in event-related theta power between ASD and TD adolescents in the previous unimodal analysis correspond to BOLD differences within the same regions. Given the uncertain spatial precision associated with aMEG findings (Lütkenhöner, 2003) and with transformation from surface to volumetric space, ROIs from the Schaefer-400 atlas (Schaefer et al., 2018) that most closely aligned with the aMEG-derived ROIs were identified as volumetric aMEG-derived ROIs (Fig. 1).

2.7.2. fMRI

A one-sample linear contrast (SW + AW + PW > Null) across all ASD and TD participants was used to identify ROIs from fMRI data. Four additional participants with usable fMRI but no MEG data were included in the ROI identification sample (Supplemental Table S3). ASD and TD participants were combined in this step. Note that ROIs determined for ASD and TD separately by group were largely similar. 3dMEMA was

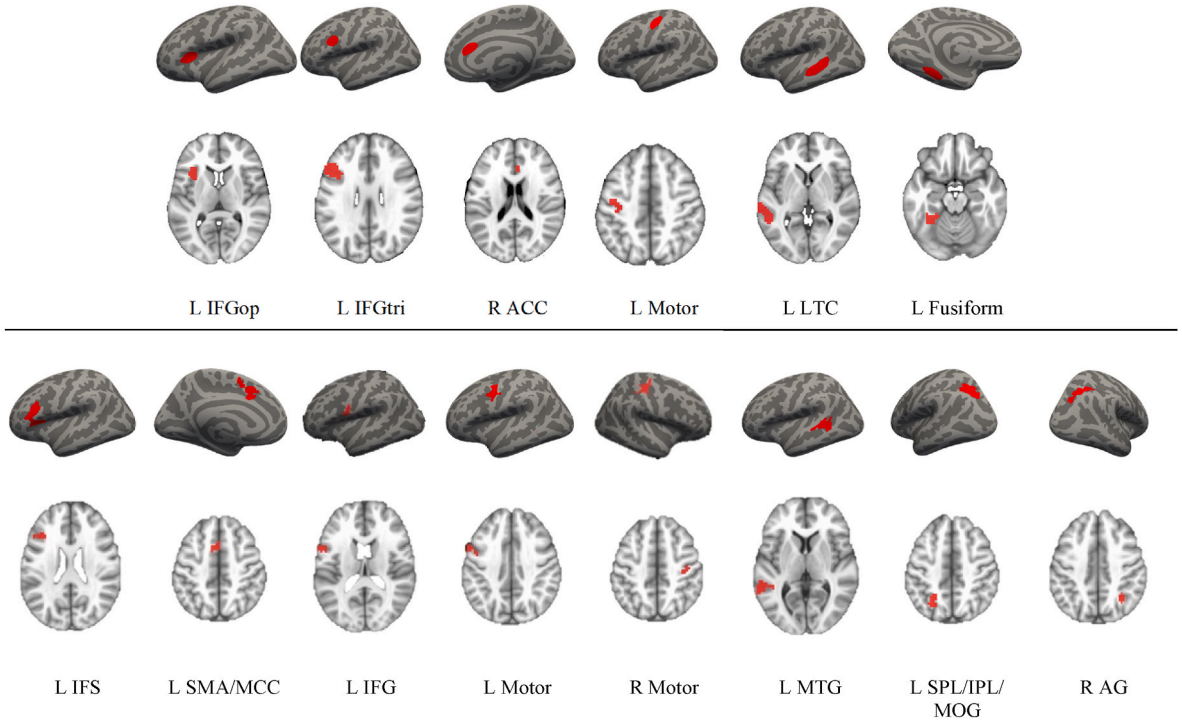

Fig. 1. aMEG-derived and fMRI-derived ROIs in surface and volumetric space. *Note*: aMEG-derived surface space ROIs depicted in top row and volumetric ROIs in second row. Volumetric ROIs that closely aligned with aMEG-derived surface space ROIs were selected from the Schaefer-400 atlas. aMEG-derived ROIs: left inferior frontal gyrus pars opercularis (L IFGop), left inferior frontal gyrus pars triangularis (L IFGtri), right anterior cingulate cortex (R ACC), left precentral gyrus (L Motor), left lateral temporal cortex (L LTC), and left fusiform gyrus. fMRI-derived surface space ROIs depicted in third row and volumetric ROIs in fourth row. fMRI-derived ROIs: left inferior frontal sulcus (L IFS); left SMA and middle cingulate cortices (L SMA/MCC); left inferior frontal gyri (L IFG); left precentral gyrus (L Motor); right precentral gyrus (R Motor); left middle temporal gyrus (L MTG); left superior parietal, inferior parietal, and middle occipital cortices (L SPL/IPL/MOG); right angular gyrus (R AG).

used to perform a mixed-effects multilevel analysis (MEMA; Chen et al., 2012) for selection of ROIs, while controlling for age, RMSD, and task accuracy. As the current version of 3dMEMA does not support permutation testing for cluster-correction, randomization and permutation simulation were performed using 3dttest++ to obtain cluster sizes with alpha $\leq$.05 on the same contrast (SW + AW + PW > Null). Clusters of increased activity in $\geq$ 56 contiguous voxels at $p \leq .001$, with most from more stringent thresholds, resulted in eleven fMRI-derived ROIs. These fMRI-derived ROIs were then transformed into surface-space ROIs using FreeSurfer (Version 7.1.1). For three ROIs, (Rolandic operculum, postcentral gyrus, and temporal pole), aMEG data could not be extracted after transformation to surface space due to ROI fragmentation caused by the transformation process, or an insufficient number of vertices required for the extraction of theta power. This resulted in eight fMRI-derived ROIs with $\geq$ 524 vertices (Fig. 1, Supplemental Table S4). ROIs were dilated to a minimum degree to permit aMEG data extraction from non-fragmented ROIs. For details, see Supplemental Table S5.

2.8. Data extraction and analysis

The goal of ROI identification was to derive ROIs from areas with the strongest activation effects related to the lexical decision task for: (1) event-related theta power from MEG scans, and (2) BOLD response from fMRI scans.

For MEG, the signal sequence was segmented based on stimulus-presentation triggers denoting zero time point for each trial. Trials were epoched from −300 to 1100 ms and baseline-corrected. Artifact-free trials with correct responses were analyzed with Morlet waves to estimate event-related theta total power averaged across 4–7 Hz at each location on the cortical surface, and presented as percent change from the baseline. MEG theta activity progressed in the posterior-to-anterior direction from sensory-specific to supramodal regions in accordance with the expected spatio-temporal processing stages. Time windows of interest were determined based on the largest theta activity across all participants for each processing stage. For each ROI, the time window of maximal event-related increase in theta power (compared with baseline) was analyzed, as previously reported by You et al. (2020). More specifically, the time windows and the corresponding regions were as follows: 150–200 ms (fusiform cortex), 250–350 ms (lateral temporal cortex), 450–650 ms (inferior frontal gyrus, lateral temporal cortex), and 700–1000 ms (anterior cingulate cortex, inferior frontal gyrus, motor cortex). For determination of MEG-derived ROIs and extraction of theta power age, sex, and handedness were not included in the model. An identical process was used to identify the MEG time windows to be analyzed for the fMRI-derived ROIs.

BOLD beta coefficients were extracted for each participant, ROI, and word condition (compared with baseline). Two (Group: ASD vs. TD) x 3 (Word Condition: SW vs. AW vs. PW) ANOVAs were used to test for the effects of group, word condition, and the interaction on event-related theta power and BOLD signal in the two sets of ROIs. Significant results from the ANOVAs were followed up with Tukey post hoc analyses to examine pairwise comparisons. Pearson partial correlations, controlling for age and fMRI RMSD, were used to examine the relationship between BOLD beta coefficients and event-related theta power in aMEG- and fMRI-derived ROIs by group.

3. Results

3.1. Event-related theta power

For aMEG-derived ROIs, a 2 x 3 ANOVA revealed a significant main effect of group with increased event-related theta power in the ASD group compared to the TD group in the following ROIs (Fig. 2A): L fusiform for the 150–200 ms time window ($F(1, 162) = 5.57$, $p = .02$), R

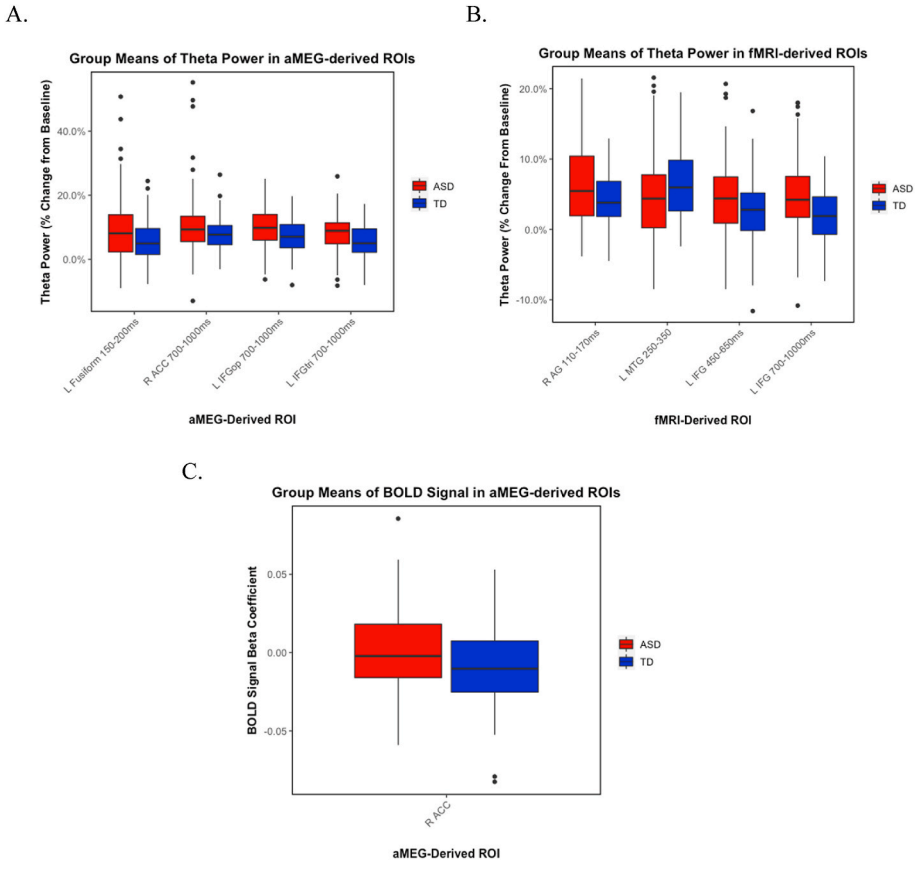

Fig. 2. Significant differences in theta power and BOLD signal in aMEG- and fMRI-derived ROIs *Note.* Mean percent change from baseline in event-related theta power (top**; A and B**) and BOLD signal (bottom**; C)** by group for ROIs with significant group differences. Fig. 2A – Theta power was significantly increased in ASD group compared to TD group for aMEG-derived ROIs: L fusiform for the 150–200 ms time window, R ACC for the 700–1000 ms time window, L IFGop for the 700–1000 ms time window, and L IFGtri for the 700–1000 ms time window. Fig. 2B – Theta power was significantly increased in ASD group compared to TD group for fMRI-derived ROIs: R AG for the 110–170 ms time window, L IFG for the 450–650 ms time window, and L IFG for the 700–1000 ms time window. Fig. 2C – Theta power was significantly increased in TD group compared to ASD group for fMRI-derived ROI L MTG for the 250–350 ms time window. BOLD signal was significantly increased in aMEG-derived ROI, R ACC, for ASD group compared to TD group. There were no group differences for BOLD signal in fMRI-derived ROIs. ASD = autism spectrum disorder. L IFG = left inferior frontal gyri. L IFGop = left inferior frontal gyrus pars opercularis. L IFGtri = left inferior frontal gyrus pars triangularis. L MTG = left middle temporal gyrus. ms = millisecond. R ACC = right anterior cingulate cortex. R AG = right angular gyrus. ROI = region-of-interest. TD = typically developing.

ACC for the 700–1000 ms time window ($F(1, 162) = 5.11$, $p = .03$), L IFGop for the 700–1000 ms time window ($F(1, 162) = 10.00$, $p = .002$), and L IFGtri for the 700–1000 ms time window ($F(1, 162) = 7.05$, $p = .009$). The ANOVA also revealed a significant main effect of word condition for event-related theta power in L IFGop for the 450–650 ms time window ($F(2, 162) = 7.39$, $p = .0009$), L IFGtri for the 450–650 ms time window ($F(2, 162) = 9.64$, $p = .0001$), and L LTC for the 450–650 ms time window ($F(2, 162) = 5.00$, $p = .008$). Tukey post hoc tests revealed significantly increased theta power for SW compared to AW [L IFGtri for the 450–650 ms time window ($p = .01$)], and for AW compared to PW [L IFGop for the 450–650 ms time window ($p = .001$), L IFGtri for the 450–650 ms time window ($p = .001$), and L LTC for the 450–650 ms time window ($p = .007$)] conditions. No significant interaction between group and word condition was identified for theta power in the aMEG-derived ROIs (Table 2; Supplemental Figure S1).

In fMRI-derived ROIs, a significant main effect of group (ASD > TD) for theta power was detected (Fig. 2B) in R AG for the 110–170 ms time window ($F(1, 162) = 7.16$, $p = .008$) and in L IFG for the 450–650 ms ($F(1, 162) = 5.01$, $p = .03$) and 700–1000 ms time windows ($F(1, 162) = 14.15$, $p = .0002$). An inverse effect of significantly greater theta power in the TD compared to the ASD group was observed in L MTG for the 250–350 ms time window ($F(1, 162) = 4.69$, $p = .03$). Significant main effects of word condition included: L IFS for the 450–650 ms time window ($F(2, 162) = 10.66$, $p < .0001$), L SMA/MCC for the 450–650 ms time window ($F(2, 162) = 4.65$, $p = .01$), L IFG for the 450–650 ms time window ($F(2, 162) = 4.75$, $p = .009$), L Motor for the 450–650 ms time window ($F(2, 162) = 5.93$, $p = .003$), L IFG for the 700–1000 ms time window ($F(2, 162) = 4.57$, $p = .01$), and R motor for the 700–1000 ms time window ($F(2, 162) = 20.95$, $p < .0001$). Tukey post hoc tests showed theta power was significantly increased for SW [L IFG for the 700–1000 ms time window ($p = .02$) and R motor for the 700–1000 ms time window ($p = .001$)] and AW [L IFS for the 450–650 ms time window ($p = .001$), L SMA/MCC for the 450–650 ms time window ($p = .008$), L IFG for the 450–650 ms time window ($p = .01$), L motor for the 450–650 ms time window ($p = .004$), and R motor for the 700–1000 ms time window ($p = .001$)] conditions when compared to PW condition. Theta power was significantly increased for AW when compared to SW in L IFS for the 450–650 ms time window ($p = .05$) and L motor for the 450–650 ms time window ($p = .02$). A significant interaction was found between group and word condition for L IFG for the 700–1000 ms time window ($F(2,162) = 3.08$, $p = .05$). Tukey post hoc analyses showed that theta power was significantly increased in the ASD group compared to the TD group for both SW ($p = .03$) and AW ($p = .02$) conditions in L IFG for the 700–1000 ms time window (Table 2; Supplemental Figure S1).

3.2. BOLD signal

For aMEG-derived ROIs, a 2 x 3 ANOVA showed a significant main effect of group, with increased BOLD signal for the ASD group compared to the TD group for BOLD signal in R ACC ($F(1, 162) = 4.80$, $p = .03$; Fig. 2C). There were significant main effects of word condition in L fusiform ($F(2, 162) = 25.19$, $p < .0001$), L LTC ($F(2, 162) = 10.61$, $p < .0001$), L IFGop ($F(2, 162) = 8.35$, $p = .0004$), L IFGtri ($F(2, 162) = 4.04$, $p = .02$), and L Motor ($F(2, 162) = 7.92$, $p = .0005$). Tukey post hoc tests showed significantly increased BOLD signal for SW compared to AW [L fusiform ($p = .001$), L LTC ($p = .001$), L IFGop ($p = .001$), and L IFGtri ($p = .01$)] and compared to PW [L fusiform ($p = .001$), L LTC ($p = .008$), and L IFGop ($p = .005$)]. The BOLD signal was also increased for the PW condition compared to AW for L motor ($p = .001$). No significant interaction between group and word condition was identified for BOLD signal in the aMEG-derived ROIs (Table 2; Supplemental Figure S2).

For fMRI-derived ROIs, there was no significant main effect of group for BOLD signal. There was a significant main effect of word condition for L SPL/IPL/MOG ($F(2, 162) = 10.65$, $p < .0001$), R AG ($F(2, 162) = 4.49$, $p = .01$), L IFG ($F(2, 162) = 6.89$, $p = .001$), L MTG ($F(2, 162) = 12.16$, $p < .0001$), L IFS ($F(2, 162) = 8.17$, $p = .0400$), L SMA/MCC ($F(2, 162) = 24.00$, $p < .0001$), L motor ($F(2, 162) = 10.76$, $p < .0001$), and R motor ($F(2, 162) = 69.48$, $p < .0001$). Results of Tukey post hoc analyses showed significantly increased BOLD signal for SW compared to AW [L SPL/IPL/MOG ($p = .001$), R AG ($p = .01$), L IFG ($p = .001$), L MTG ($p = .001$), L IFS ($p = .001$), L SMA/MCC ($p = .001$), L motor ($p = .001$), and R motor ($p = .001$)] and SW compared to PW [L SPL/IPL/MOG ($p = .005$), L IFG ($p = .03$), L MTG ($p = .001$), L SMA/MCC ($p = .001$), and R motor ($p = .001$)]. BOLD signal was significantly greater for PW compared to AW in L motor ($p = .002$) and for AW compared to PW in R motor ($p = .001$). A significant interaction was found between group and word condition for L IFS ($F(2,162) = 3.18$, $p = .04$). Tukey post hoc analyses for L IFS did not show significant group differences for any of the word conditions (Table 2; Supplemental Figure S2).

3.3. MEG-fMRI correlations

None of the partial correlations (controlling for fMRI RMSD and age) between theta power and BOLD signal survived FDR-adjustment (alpha = .05; Benjamini and Hochberg, 1995), with only a few reaching an uncorrected threshold $p \leq .05$. For MEG-derived ROIs (Supplemental Table S6; Figure S3), correlations were found in the TD group in L LTC for the 250–350 ms time window for AW ($r(19) = -.46$, $p = .05$), and in the ASD group in R ACC for the 700–1000 ms time window for PW ($r(27) = 0.46$, $p = .02$). For fMRI-derived ROIs, a correlation was found in the TD group in L MTG for the 250–350 ms time window for the AW condition ($r(27) = -.62$, $p = .004$; Supplemental Table S7; Figure S3). To account for any effect of time between scans on the relationship, partial correlations were also examined with the addition of the number of days between scans as a covariate. The length of time between fMRI and MEG scans did not have a significant impact on the results of the partial correlation.

3.4. Supplementary analyses

Three sets of supplementary analyses were conducted to account for outliers, participants with high motion, and those with >150 days between fMRI and MEG scans. See supplement for additional analyses (Supplemental Tables S8-S18; Figures S4-S9).

4. Discussion

In this study, we examined the relation between event-related theta power measured with aMEG and fMRI BOLD signal during lexicosemantic processing in adolescents with ASD and TD peers. We found that correspondence between task related changes in BOLD signal and theta power was generally weak. Atypically increased theta power in ASD across several ROIs was mostly not reflected in corresponding BOLD group differences, suggesting that the two imaging methods are differentially sensitive to at least some ASD-specific alterations and capturing different aspects of the neural signal.

4.1. Task-induced signal changes in MEG and fMRI

Marinkovic et al. (2012) previously tested this lexicosemantic task in neurotypical adults using aMEG data. ROIs from that study included the occipital cortex, left lateral and inferior frontal regions, anterior cingulate, and motor cortex. Most of the ROIs in the present study overlap with these previous findings. Refer to the supplement for additional details on the background literature on identified ROIs and their relation to the different processing stages involved in the task.

Multiple frontal and temporal ROIs (both aMEG and fMRI-derived) showed greater increase in event-related theta power in the ASD than the TD group. This is consistent with the overall pattern of increased theta power reported in You et al. (2020), which included a smaller, partially overlapping sample. However, only one region (R ACC) showed a concordant group difference for the BOLD signal, whereas no group

Table 2
ANOVA comparisons of event-related theta power and BOLD signal.

Theta Power in aMEG-derived ROIs							
Time Window (ms)	ROI	Group		Condition		Group x Condition	
		F(1,162)	*p*	*F*(1,162)	*p*	*F*(1,162)	*p*
150–200	L Fusiform	5.57	0.02*	0.09	0.91	0.11	0.90
250–350	L LTC	1.96	0.16	0.96	0.39	0.45	0.64
450–650	L IFGop	0.88	0.35	7.39	0.0009**	1.50	0.23
	L IFGtri	2.37	0.13	9.64	0.0001***	1.09	0.34
	L LTC	0.00005	0.99	5.00	0.008**	1.70	0.19
700–1000	R ACC	5.11	0.03*	1.61	0.20	1.02	0.36
	L IFGop	10.00	0.002**	1.91	0.15	1.39	0.25
	L IFGtri	7.05	0.01**	1.20	0.31	2.70	0.07
	L Motor	2.84	0.09	2.48	0.09	1.12	0.33
Theta Power in fMRI-derived ROIs							
Time Window (ms)	ROI	Group		Condition		Group x Condition	
		F(1,162)	*p*	*F*(1,162)	*p*	*F*(1,162)	*p*
110–170	L SPL/IPL/MOG	3.06	0.08	0.04	0.96	0.03	0.97
	R AG	7.08	0.008**	0.68	0.51	0.07	0.93
250–350	L IFG	0.49	0.48	0.94	0.39	0.69	0.50
	L MTG	4.69	0.03*	0.47	0.62	0.11	0.89
450–650	L IFS	2.09	0.15	10.66	<0.0001***	1.67	0.19
	L SMA/MCC	0.95	0.33	4.65	0.01*	0.38	0.69
	L IFG	5.01	0.03*	4.75	0.009**	0.24	0.79
	L Motor	1.08	0.30	5.93	0.003**	1.14	0.32
700–1000	L IFG	14.15	0.0002***	4.57	0.01*	3.08	0.05*
	R Motor	3.07	0.08	20.95	<0.0001***	0.71	0.49
BOLD Signal in aMEG-derived ROIs							
ROI	Group			Condition		Group x Condition	
	F(1,162)	*p*		*F*(1,162)	*p*	*F*(1,162)	*p*
L Fusiform	0.28	0.60		25.19	<0.0001***	2.80	0.06
L LTC	1.49	0.22		10.61	<0.0001***	0.82	0.44
L IFGop	0.58	0.45		8.35	0.0004***	1.46	0.24
L IFGtri	0.64	0.42		4.04	0.02*	2.13	0.12
R ACC	4.80	0.03*		1.42	0.25	0.80	0.45
L Motor	1.19	0.28		7.92	0.0005***	0.30	0.74
BOLD Signal in fMRI-derived ROIs							
ROI	Group			Condition		Group x Condition	
	F(1,162)	*p*		*F*(1,162)	*p*	*F*(1,162)	*p*
L SPL/IPL/MOG	0.06	0.81		10.65	<0.0001***	1.78	0.17
R AG	0.04	0.84		4.49	0.01**	0.96	0.39
L IFG	0.03	0.85		6.89	0.001**	0.07	0.93
L MTG	2.57	0.11		12.16	<0.0001***	0.82	0.44
L IFS	0.001	0.97		8.17	0.0004***	3.18	0.04*
L SMA/MCC	0.52	0.47		24.00	<0.0001***	1.00	0.37
L Motor	0.01	0.91		10.76	<0.0001***	0.09	0.91
R Motor	0.01	0.93		69.48	<0.0001***	0.70	0.50

Note: 2 x 3 ANOVA tests looked at the effect of group (ASD, TD) and word condition (SW, AW, PW) and the interaction on event-related theta power and BOLD beta coefficients in both set of ROIs. Group differences in theta power were observed across multiple regions for both sets of ROIs. One group difference in BOLD signal was observed. The interaction was mostly nonsignificant, except for theta power in fMRI-derived ROI L IFG for the 700–1000 ms time window. * denotes $p \leq .05$, ** $p \leq .01$, *** $p \leq .001$.

ASD = autism spectrum disorder.
AW = animal word.
L IFG = left inferior frontal gyri.
L IFGop = left inferior frontal gyrus pars opercularis.
L IFGtri = left inferior frontal gyrus pars triangularis.
L IFS = left inferior frontal sulcus.
L LTC = left lateral temporal cortex.
L MTG = left middle temporal gyrus.
L SMA/MCC = left SMA and middle cingulate cortices.
L SPL/IPL/MOG = left superior parietal, inferior parietal, and middle occipital cortices.
ms = millisecond.
PW = pseudoword
R ACC = right anterior cingulate cortex.
R AG = right angular gyrus.
ROI = region-of-interest.
SW = standard word.
TD = typically developing.

differences in BOLD signal were detected for any other of the 14 ROIs.

It is interesting that both theta power and BOLD signal in the ACC were significantly greater in the ASD group compared to the TD group. The ACC is known to play a role in decision making, as described above (Kovacevic et al., 2012; Marinkovic et al., 2012; Posner et al., 2007; Ruff et al., 2008). Atypically increased activation in the ASD group in this region may be due to greater attentional engagement in adolescents with ASD during the final stage of task processing. Participants needed to decide what word category the presented word falls in, recall what finger to press for that word category, and then execute the button press or inhibit a response in case of a pseudoword. The planning and organization required during this step calls on the individual's executive functioning skills. It has been widely found that individuals with ASD have deficits in this domain, with many studies pointing to the relationship between executive functioning and the ACC in ASD (Braconnier and Siper, 2021; Demetriou et al., 2019; Hill, 2004; May and Kana, 2020; Zhang et al., 2020).

The lack of group differences in BOLD signal for a majority of the ROIs appears to be in contrast to previous reports of atypical BOLD signal in ASD during lexicosemantic processing (Gaffrey et al., 2007; Harris et al., 2006; Just et al., 2004; Knaus et al., 2017; Lo et al., 2013; Moseley et al., 2013; Sahyoun et al., 2010; Shen et al., 2012). Several reasons may account for this finding in our study. fMRI-derived ROIs were based on data pooled from both ASD and TD groups. Given our study's focus on the relation between BOLD signal and theta power, fMRI-derived ROIs were limited to those showing the greatest task-induced increases across the entire sample. However, as suggested by some previous lexicosemantic studies, atypical activity patterns may occur in regions *outside* the neurotypical language network (Gaffrey et al., 2007; Gao et al., 2019; Kana et al., 2006; Knaus et al., 2008; Shen et al., 2012). Therefore, heterogeneity and ASD variants with diverging patterns of atypical language networks may obscure differences from TD comparison groups (Gao et al., 2019; Lombardo et al., 2019). Notably, within some of these regions of shared activation, group differences in event-related theta power could nonetheless be detected.

4.2. Relation between BOLD signal and theta power

The results of this study show a significant correlation in the positive direction between theta power and BOLD signal in the ACC for the ASD group. As described above, the ACC plays an important role in cognitive control, decision making, and attention (Carter and van Veen, 2007; Heilbronner and Hayden, 2016; Posner et al., 2007; Ruff et al., 2008). Theta power is also linked to these domains (Klimesch, 1999; Kovacevic et al., 2012; Marinkovic et al., 2012). Previous studies suggest that the ACC may be a a major generator of theta oscillation (Holroyd and Umemoto, 2016; Kouijzer et al., 2010; Luu and Tucker, 2001; Rajan et al., 2019; Tsujimoto et al., 2006).

Aside from the ACC, no other distinct pattern was detected in the relationship between event-related BOLD and theta signal changes. One might expect to see some correspondence between BOLD signal and theta power, since each measure is considered an index of choice in studies testing for task- or stimulus-related regional 'activation' (Audrain et al., 2020; Bakker-Marshall et al., 2018; Bastiaansen et al., 2005; Begus and Bonawitz, 2020; Gaffrey et al., 2007; Halgren et al., 2015; Harris et al., 2006; Just et al., 2004; Knaus et al., 2017; Kovacevic et al., 2012; Lo et al., 2013; Marinkovic et al., 2012, 2019; Moseley et al., 2013; Pu et al., 2020; Sahyoun et al., 2010; Shen et al., 2012). Indeed, event-related theta oscillations are particularly relevant to the double-duty lexical decision task employed in the current study that combined demands on both lexicosemantic processing and cognitive control. It has been well established that event-related theta power is sensitive to the retrieval of lexicosemantic information (Bastiaansen et al., 2008; Halgren et al., 2015), cognitive control (Cavanagh and Frank, 2014; Correas et al., 2019; Kovacevic et al., 2012), and the integration of task-relevant representations across long-range functional networks (Bastiaansen and Hagoort, 2006; Halgren et al., 2015; Marinkovic et al., 2012).

To critically evaluate the relationship between fMRI and MEG, it is important to understand neurovascular coupling, that is, how local neuronal activity relates to increases in blood flow. For fMRI, the BOLD effect – conventionally considered the sole available (though indirect) assay of neuronal activity changes – measures changes in blood oxygenation that begin within 500 ms of stimulus onset and peak with a c.5 s delay (Hillman, 2014). When a stimulus is presented, there is an increase in oxygenation in activated brain regions, resulting in a local BOLD signal increase (Buxton, 2009; Hillman, 2014). The relationship between hemodynamics and brain activation has allowed the field to use vascular changes as an index of neural activity. Other metabolic and physiological processes that may impact the spatiotemporal processes of the BOLD signal include differences in the timing of blood vessel dilation and constriction, residual neurochemical changes post stimulus, and changes in the amount of neurotransmitters (Hillman, 2014). The relationship between neurovascular coupling and BOLD signal changes also depends on region and cortical depth (Devonshire et al., 2012; Goense et al., 2012). Neurovascular coupling differences may exist in ASD due to neurophysiological changes such as decreased inhibition that can increase blood flow and nitric oxide activity, which can in turn lead to an increased hemodynamic response (Reynell and Harris, 2013).

Unlike the reliance on hemodynamics in fMRI, the MEG signal is directly sensitive to neuronal activity, with a temporal resolution at the millisecond level (Ahlfors and Mody, 2019; Baillet, 2017). Previous work in monkeys has shown a strong relationship between MEG and local field potentials (LFP), providing support that MEG activity measures postsynaptic events (Hall et al., 2014). Neural oscillations can be analyzed in time domain by averaging event-related fields per time unit, or in time-frequency domain by decomposing oscillatory signals into different frequency bands in a time-sensitive manner. These analyses provide different insights into the underlying spatio-temporal signal characteristics (Marinkovic et al., 2012, 2014). Despite the obvious benefits of MEG, such as its direct sensitivity to neural activity with excellent temporal resolution, its spatial estimates depend on the source modeling used to solve the inverse problem (Dale and Halgren, 2001). In the present study, we employed an aMEG method that combines distributed source modeling of the MEG signal with structural MRI. It constrains inverse solutions to each participant's cortical mantle based on real-shape head models.

The lack of relation between the two measures in the current study is not surprising given inconsistent findings in previous multimodal task-based neuroimaging studies reporting both positive and negative correlations (Ekstrom et al., 2009; Meltzer et al., 2007; Scheeringa et al., 2009; Scheeringa and Fries, 2019; Singh et al., 2002; Winterer et al., 2007). Singh et al. (2002) reported an inverse relationship between fMRI response and event-related desynchronizations in the 5–15 Hz band, which includes theta power. However, this study included a small sample, with participants differing between the two modalities, and did not specifically focus on the 4–7 Hz range. A negative correlation between BOLD signal and theta power (measured with EEG) was also found within the default mode network in two studies of neurotypical adults (Meltzer et al., 2007; Scheeringa et al., 2009). By contrast, the relationship between BOLD signal and event-related theta power during a visual decision task was found to be positive in motor cortex, but negative in ACC (Winterer et al., 2007). Although some of the seemingly inconsistent results may be attributed to differences in task and regions tested, the relation between BOLD signal and theta power is clearly complex and incompletely understood, and findings in ASD from the current study are therefore not unexpected. Such a complex and seemingly intransparent relationship can be viewed in a positive light, according to Hari and Salmelin (2012) who argue that differences in findings may be more informative than similarities. Indeed, as fMRI and MEG detect neural activity in fundamentally different ways, differential findings may be considered complementary rather than inconsistent.

4.3. Limitations

fMRI analyses are conventionally volume-based, whereas they are surface-based in MEG. Due to some inherent limitations of volume to surface transformation, a few fMRI-derived ROIs could not be transformed into usable surface ROIs. Additionally, although MEG analyses focused on theta power in the present study given the established sensitivity of this frequency band to language processing and cognitive control, the MEG signal is inherently oscillatory and multiplexed, and future investigations of changes in other frequency bands may be useful. Slight differences in task presentation between MEG and fMRI scans were unavoidable due to differences in neuroimaging techniques, such as the need for null trials and jittering in fMRI.

While there are potential confounds that can lead to differences between scans over time, such as seasonal changes, menstrual cycles, or circadian rhythms, efforts were taken to reduce the possible impact of external circumstances. The number of days between MEG and fMRI scans was kept at a minimum to limit effects of maturational changes in adolescents. A large majority of the participants (85% ASD, 78% TD) in the analysis completed scans within a 3-month time frame. Although the results presented here are from a group of participants with a scan interval range of 1–252 days, supplemental analyses conducted in participants who completed the scans within 150 days did not alter the overall findings. In this supplemental analysis most participants (90% ASD, 82% TD) were in the 3-month timeframe. There was no significant difference in scan intervals between ASD and TD groups. ($t(53) = -1.31$, $p = .19$). When days between scans was added as a covariate, there was no impact on the correlation between BOLD signal and event-related theta power. Additionally, most of the participants were above 15 years of age, rather than in a younger range when the brain is more rapidly developing and changing. Finally, due to lengthy fMRI and MEG scans and the moderately challenging lexicosemantic task, our ASD sample was limited to relatively high-functioning adolescents and findings may therefore not represent the broader autism spectrum, including minimally verbal and nonverbal individuals.

5. Conclusion

Comparing two metrics of choice for the detection of brain regional activity changes during lexicosemantic decision in adolescents with ASD and TD peers, we found no clear relationship between event-related fMRI BOLD signal and aMEG theta power. This indicates that reports of atypical “activation” patterns in ASD can only be interpreted with respect to the specific neuroimaging modality used. Group differences detected with aMEG, but not fMRI, further suggest that some neurofunctional differences in ASD may occur at the level of dynamic processing that is not detected at the limited temporal resolution of the hemo-dynamic response in fMRI. More generally, differential findings emphasize the need for integration between imaging modalities that have thus far been implemented largely in isolation in ASD research and beyond.

Funding sources

This work has been funded by the National Institutes of Health [Integrity and Dynamic Processing Efficiency of Networks in ASD, R01MH101173-01] and the National Institutes of Health Training Grant [Training in Advanced Data Analytics for Behavioral and Social Sciences Research, 5T32MH122376].

Declaration of competing interest

The authors declare that they have no known competing financial interests or personal relationships that could have appeared to influence the work reported in this paper.

Appendix A. Supplementary data

Supplementary data to this article can be found online at https://doi.org/10.1016/j.ynirp.2022.100134.

References

Ahlfors, S.P., Mody, M., 2019. Overview of MEG. Organ. Res. Methods 22 (1), 95–115. https://doi.org/10.1177/1094428116676344.

American Psychiatric Association, 2013. Diagnostic and Statistical Manual of Mental Disorders. American Psychiatric Association. https://doi.org/10.1176/appi.books.9780890425596.

Audrain, S.P., Urbain, C.M., Yuk, V., Leung, R.C., Wong, S.M., Taylor, M.J., 2020. Frequency-specific neural synchrony in autism during memory encoding, maintenance and recognition. Brain Communications 2 (2). https://doi.org/10.1093/braincomms/fcaa094.

Baillet, S., 2017. Magnetoencephalography for brain electrophysiology and imaging. Nat. Neurosci. 20 (3), 327–339. https://doi.org/10.1038/nn.4504.

Bakker-Marshall, I., Takashima, A., Schoffelen, J.M., Van Hell, J.G., Janzen, G., McQueen, J.M., 2018. Theta-band oscillations in the middle temporal gyrus reflect novel word consolidation. J. Cognit. Neurosci. 30 (5), 621–633. https://doi.org/10.1162/jocn_a_01240.

Bastiaansen, M.C.M., Oostenveld, R., Jensen, O., Hagoort, P., 2008. I see what you mean: theta power increases are involved in the retrieval of lexical semantic information. Brain Lang. 106 (1), 15–28. https://doi.org/10.1016/j.bandl.2007.10.006.

Bastiaansen, M.C., van der Linden, M., ter Keurs, M., Dijkstra, T., Hagoort, P., 2005. Theta Responses Are Involved in Lexical-Semantic Retrieval during Language Processing.

Bastiaansen, M., Hagoort, P., 2006. Oscillatory neuronal dynamics during language comprehension. Prog. Brain Res. 159 (6), 179–196. https://doi.org/10.1016/S0079-6123(06)59012-0.

Bavin, E.L., Prendergast, L.A., Kidd, E., Baker, E., Dissanayake, C., 2016. Online processing of sentences containing noun modification in young children with high-functioning autism. https://doi.org/10.1111/1460-6984.12191, 51(2), 137-147.

Beaton, L.E., Azma, S., Marinkovic, K., 2018. When the brain changes its mind: oscillatory dynamics of conflict processing and response switching in a flanker task during alcohol challenge. PLoS One 13 (1), e0191200. https://doi.org/10.1371/journal.pone.0191200.

Beery, K.E., Buktenica, N.A., Beery, N.A., 2010. The Beery–Buktenica Developmental Test of Visual–Motor Integration: Administration, Scoring, and Teaching Manual. Sixth Edit). Pearson.

Begus, K., Bonawitz, E., 2020. The rhythm of learning: theta oscillations as an index of active learning in infancy. Dev. Cognitive Neurosci. 45, 100810 https://doi.org/10.1016/j.dcn.2020.100810.

Benjamini, Y., Hochberg, Y., 1995. Controlling the false Discovery rate : a practical and powerful approach to multiple testing. J. Roy. Stat. Soc. 57 (1), 289–300.

Bolton, T.A.W., Morgenroth, E., Preti, M.G., Van De Ville, D., 2020. Tapping into multi-faceted human behavior and psychopathology using fMRI brain dynamics. Trends Neurosci. 43 (9), 667–680. https://doi.org/10.1016/j.tins.2020.06.005.

Boucher, J., 2003. Language development in autism. Int. Congr. 1254, 247–253. https://doi.org/10.1016/s0531-5131(03)00976-2.

Boucher, J., 2012. Research review: structural language in autistic spectrum disorder - characteristics and causes. In: Journal of Child Psychology and Psychiatry and Allied Disciplines, vol. 53. John Wiley & Sons, Ltd, pp. 219–233. https://doi.org/10.1111/j.1469-7610.2011.02508.x. Issue 3.

Braconnier, M.L., Siper, P.M., 2021. Neuropsychological assessment in autism spectrum disorder. Curr. Psychiatr. Rep. 23 (10), 63. https://doi.org/10.1007/s11920-021-01277-1.

Brysbaert, M., New, B., 2009. Moving beyond Kučera and Francis: a critical evaluation of current word frequency norms and the introduction of a new and improved word frequency measure for American English. Behav. Res. Methods 41 (4), 977–990. https://doi.org/10.3758/BRM.41.4.977.

Buxton, R.B., 2009. Introduction to Functional Magnetic Resonance Imaging: Principles and Techniques, second ed. Cambridge University Press.

Carter, C.S., van Veen, V., 2007. Anterior cingulate cortex and conflict detection: an update of theory and data. Cognit. Affect Behav. Neurosci. 7 (4), 367–379. https://doi.org/10.3758/CABN.7.4.367.

Cavanagh, Frank, M.J., 2014. Frontal theta as a mechanism for affective and effective control. Trends Cognit. Sci. 18 (8), 414–421. https://doi.org/10.1016/j.tics.2014.04.012.

Chen, G., Saad, Z.S., Nath, A.R., Beauchamp, M.S., Cox, R.W., 2012. FMRI group analysis combining effect estimates and their variances. Neuroimage 60 (1), 747–765. https://doi.org/10.1016/j.neuroimage.2011.12.060.

Correas, A., López-Caneda, E., Beaton, L., Rodríguez Holguín, S., García-Moreno, L.M., Antón-Toro, L.F., Cadaveira, F., Maestú, F., Marinkovic, K., 2019. Decreased event-related theta power and phase-synchrony in young binge drinkers during target detection: an anatomically-constrained MEG approach. J. Psychopharmacol. 33 (3), 335–346. https://doi.org/10.1177/0269881118805498.

Cox, R.W., 1996. AFNI: software for analysis and visualization of functional magnetic resonance neuroimages. Comput. Biomed. Res. 29 (3), 162–173. https://doi.org/10.1006/cbmr.1996.0014.

Dale, A.M., Halgren, E., 2001. Spatiotemporal mapping of brain activity by integration of multiple imaging modalities. Curr. Opin. Neurobiol. 11 (2), 202–208. https://doi.org/10.1016/S0959-4388(00)00197-5.

Dale, Anders M., Fischl, B., Sereno, M.I., 1999. Cortical surface-based analysis: I. Segmentation and surface reconstruction. Neuroimage 9 (2), 179–194. https://doi.org/10.1006/nimg.1998.0395.

Dale, Anders M., Liu, A.K., Fischl, B.R., Buckner, R.L., Belliveau, J.W., Lewine, J.D., Halgren, E., 2000. Dynamic statistical parametric mapping: combining fMRI and MEG for high-resolution imaging of cortical activity. Neuron 26 (1), 55–67. https://doi.org/10.1016/S0896-6273(00)81138-1.

Delorme, A., Makeig, S., 2004. EEGLAB: an open source toolbox for analysis of single-trial EEG dynamics including independent component analysis. J. Neurosci. Methods 134 (1), 9–21. https://doi.org/10.1016/j.jneumeth.2003.10.009.

Demetriou, E.A., DeMayo, M.M., Guastella, A.J., 2019. Executive function in autism spectrum disorder: history, theoretical models, empirical findings, and potential as an endophenotype. Front. Psychiatr. 10 https://doi.org/10.3389/fpsyt.2019.00753.

Devonshire, I.M., Papadakis, N.G., Port, M., Berwick, J., Kennerley, A.J., Mayhew, J.E. W., Overton, P.G., 2012. Neurovascular coupling is brain region-dependent. Neuroimage 59 (3), 1997. https://doi.org/10.1016/j.neuroimage.2011.09.050, 2006.

Ekstrom, A., Suthana, N., Millett, D., Fried, I., Bookheimer, S., 2009. Correlation between BOLD fMRI and theta-band local field potentials in the human hippocampal area. J. Neurophysiol. 101 (5), 2668–2678. https://doi.org/10.1152/jn.91252.2008.

Fischl, B., Sereno, M.I., Dale, A.M., 1999a. Cortical surface-based analysis: II. Inflation, flattening, and a surface-based coordinate system. Neuroimage 9 (2), 195–207. https://doi.org/10.1006/nimg.1998.0396.

Fischl, B., Sereno, M.I., Tootell, R.B.H., Dale, A.M., 1999. High-resolution intersubject averaging and a coordinate system for the cortical surface. Hum. Brain Mapp. 8, 272–284. https://doi.org/10.1002/(SICI)1097-0193(1999)8:4<272::AID-HBM10>3.0.CO;2-4.

Gaffrey, M.S., Kleinhans, N.M., Haist, F., Akshoomoff, N., Campbell, A., Courchesne, E., Müller, R.A., 2007. A typical participation of visual cortex during word processing in autism: an fMRI study of semantic decision. Neuropsychologia 45 (8), 1672–1684. https://doi.org/10.1016/j.neuropsychologia.2007.01.008.

Gao, Y., Linke, A., Jao Keehn, R.J., Punyamurthula, S., Jahedi, A., Gates, K., Fishman, I., Müller, R.A., 2019. The language network in autism: atypical functional connectivity with default mode and visual regions. Autism Res. 12 (9), 1344–1355. https://doi.org/10.1002/aur.2171.

Goense, J., Merkle, H., Logothetis, N.K., 2012. High-resolution fMRI reveals laminar differences in neurovascular coupling between positive and negative BOLD responses. Neuron 76 (3), 629–639. https://doi.org/10.1016/j.neuron.2012.09.019.

Gramfort, A., Luessi, M., Larson, E., Engemann, D.A., Strohmeier, D., Brodbeck, C., Parkkonen, L., Hämäläinen, M.S., 2014. MNE software for processing MEG and EEG data. Neuroimage 86, 446–460. https://doi.org/10.1016/j.neuroimage.2013.10.027.

Groen, W.B., Zwiers, M.P., van der Gaag, R.J., Buitelaar, J.K., 2008. The phenotype and neural correlates of language in autism: an integrative review. In: Neuroscience and Biobehavioral Reviews, vol. 32. Pergamon, pp. 1416–1425. https://doi.org/10.1016/j.neubiorev.2008.05.008. Issue 8.

Gurney, J.G., McPheeters, M.L., Davis, M.M., 2006. Parental report of health conditions and health care use among children with and without autism: National survey of children's health. Arch. Pediatr. Adolesc. Med. 160 (8), 825–830. https://doi.org/10.1001/archpedi.160.8.825.

Halgren, E., Kaestner, E., Marinkovic, K., Cash, S.S., Wang, C., Schomer, D.L., Madsen, J. R., Ulbert, I., 2015. Laminar profile of spontaneous and evoked theta: rhythmic modulation of cortical processing during word integration. Neuropsychologia 76, 108–124. https://doi.org/10.1016/j.neuropsychologia.2015.03.021.

Hall, E.L., Robson, S.E., Morris, P.G., Brookes, M.J., 2014. The relationship between MEG and fMRI. In: NeuroImage, vol. 102. Academic Press Inc, pp. 80–91. https://doi.org/10.1016/j.neuroimage.2013.11.005. Issue P1.

Hari, R., Salmelin, R., 2012. Magnetoencephalography: from SQUIDs to neuroscience. Neuroimage 20th anniversary special edition. Neuroimage 61 (2), 386–396. https://doi.org/10.1016/j.neuroimage.2011.11.074.

Harris, G.J., Chabris, C.F., Clark, J., Urban, T., Aharon, I., Steele, S., McGrath, L., Condouris, K., Tager-Flusberg, H., 2006. Brain activation during semantic processing in autism spectrum disorders via functional magnetic resonance imaging. Brain Cognit. 61 (1), 54–68. https://doi.org/10.1016/j.bandc.2005.12.015.

Heilbronner, S.R., Hayden, B.Y., 2016. Dorsal anterior cingulate cortex: a bottom-up view. Annu. Rev. Neurosci. 39, 149–170. https://doi.org/10.1146/annurev-neuro-070815-013952.

Hill, E.L., 2004. Executive dysfunction in autism. Trends Cognit. Sci. 8 (1), 26–32. https://doi.org/10.1016/j.tics.2003.11.003.

Hillman, E.M.C., 2014. Coupling mechanism and significance of the BOLD signal: a status report. Annu. Rev. Neurosci. 37, 161–181. https://doi.org/10.1146/annurev-neuro-071013-014111.

Holroyd, C.B., Umemoto, A., 2016. The research domain criteria framework: the case for anterior cingulate cortex. Neurosci. Biobehav. Rev. 71, 418–443. https://doi.org/10.1016/j.neubiorev.2016.09.021.

Hornung, T., Chan, W.-H., Muller, R.-A., Townsend, J., Keehn, B., 2019. Dopaminergic hypo-activity and reduced theta-band power in autism spectrum disorder: a resting-state EEG study. Int. J. Psychophysiol. 146, 101–106. https://doi.org/10.1016/j.ijpsycho.2019.08.012.Dopaminergic.

Just, M.A., Cherkassky, V.L., Keller, T.A., Minshew, N.J., 2004. Cortical activation and synchronization during sentence comprehension in high-functioning autism: evidence of underconnectivity. Brain 127 (8), 1811–1821. https://doi.org/10.1093/brain/awh199.

Kamio, Y., Robins, D., Kelley, E., Swainson, B., Fein, D., 2007. Atypical lexical/semantic processing in high-functioning autism spectrum disorders without early language delay. J. Autism Dev. Disord. 37 (6), 1116–1122. https://doi.org/10.1007/s10803-006-0254-3.

Kana, R.K., Keller, T.A., Cherkassky, V.L., Minshew, N.J., Just, M.A., 2006. Sentence comprehension in autism: thinking in pictures with decreased functional connectivity. Brain 129 (9), 2484–2493. https://doi.org/10.1093/brain/awl164.

Klimesch, W., 1999. Full-length review EEG alpha and theta oscillations reflect cognitive and memory performance: a review and analysis. Brain Res. Rev. 29, 169–195. https://doi.org/10.1016/S0165-0173(98)00056-3.

Knaus, T.A., Burns, C., Kamps, J., Foundas, A.L., 2017. Atypical activation of action-semantic network in adolescents with autism spectrum disorder. Brain Cognit. 117, 57–64. https://doi.org/10.1016/j.bandc.2017.06.004.

Knaus, T.A., Silver, A.M., Lindgren, K.A., Hadjikhani, N., Tager-Flusberg, H., 2008. fMRI activation during a language task in adolescents with ASD. J. Int. Neuropsychol. Soc. 14 (6), 967–979. https://doi.org/10.1017/S1355617708081216.

Kouijzer, M.E.J., van Schie, H.T., de Moor, J.M.H., Gerrits, B.J.L., Buitelaar, J.K., 2010. Neurofeedback treatment in autism. Preliminary findings in behavioral, cognitive, and neurophysiological functioning. Res. Autism Spectrum Disorders 4 (3), 386–399. https://doi.org/10.1016/j.rasd.2009.10.007.

Kovacevic, S., Azma, S., Irimia, A., Sherfey, J., Halgren, E., Marinkovic, K., 2012. Theta oscillations are sensitive to both early and late conflict processing stages: effects of alcohol intoxication. PLoS One 7 (8), e43957. https://doi.org/10.1371/journal.pone.0043957.

Kundu, P., Brenowitz, N.D., Voon, V., Worbe, Y., Vértes, P.E., Inati, S.J., Saad, Z.S., Bandettini, P.A., Bullmore, E.T., 2013. Integrated strategy for improving functional connectivity mapping using multiecho fMRI. Proc. Natl. Acad. Sci. U. S. A 110 (40), 16187–16192. https://doi.org/10.1073/pnas.1301725110.

Kundu, P., Inati, S.J., Evans, J.W., Luh, W.M., Bandettini, P.A., 2012. Differentiating BOLD and non-BOLD signals in fMRI time series using multi-echo EPI. Neuroimage 60 (3), 1759–1770. https://doi.org/10.1016/j.neuroimage.2011.12.028.

Kuperman, V., Stadthagen-Gonzalez, H., Brysbaert, M., 2012. Age-of-acquisition ratings for 30,000 English words. Behav. Res. Methods 44 (4), 978–990. https://doi.org/10.3758/s13428-012-0210-4.

Lachaux, J.-P., Rodriguez, E., Martinerie, J., Varela, F.J., 1999. Measuring phase synchonry in brain signals. Hum. Brain Mapp. 8, 194–208. https://doi.org/10.1002/(sici)1097-0193(1999)8:4<194::aid-hbm4>3.0.co;2-c, 1999.

Larrain-Valenzuela, J., Zamorano, F., Soto-Icaza, P., Carrasco, X., Herrera, C., Daiber, F., Aboitiz, F., Billeke, P., 2017. Theta and alpha oscillation impairments in autistic spectrum disorder reflect working memory deficit. Sci. Rep. 7 (1), 1–11. https://doi.org/10.1038/s41598-017-14744-8.

Liu, S., Cai, W., Liu, S., Zhang, F., Fulham, M., Feng, D., Pujol, S., Kikinis, R., 2015. Multimodal neuroimaging computing: a review of the applications in neuropsychiatric disorders. Brain Informatics 2 (3), 167–180. https://doi.org/10.1007/s40708-015-0019-x.

Lo, Y.C., Chou, T.L., Fan, L.Y., Gau, S.S.F., Chiu, Y.N., Tseng, W.Y.I., 2013. Altered structure-function relations of semantic processing in youths with high-functioning autism: a combined diffusion and functional MRI study. Autism Res. 6 (6), 561–570. https://doi.org/10.1002/aur.1315.

Lombardo, M.V., Lai, M.C., Baron-Cohen, S., 2019. Big data approaches to decomposing heterogeneity across the autism spectrum. Mol. Psychiatr. 24 (10), 1435–1450. https://doi.org/10.1038/s41380-018-0321-0.

Lord, C., Rutter, M., DiLavore, P.C., Risi, S., Gotham, K., Bishop, S., 2012. Autism Diagnostic Observation Schedule. Second Edi. Western Psychological Services. https://www.wpspublish.com/ados-2-autism-diagnostic-observation-schedule-second-edition.

Lütkenhöner, B., 2003. Magnetoencephalography and its achilles' heel. J. Physiol. Paris 97 (4–6), 641–658. https://doi.org/10.1016/j.jphysparis.2004.01.020.

Luu, P., Tucker, D.M., 2001. Regulating action: alternating activation of midline frontal and motor cortical networks. Clin. Neurophysiol. 112, 1295–1306. https://doi.org/10.1016/S1388-2457(01)00559-4.

Lynch, C.J., Power, J.D., Scult, M.A., Dubin, M., Gunning, F.M., Liston, C., 2020. Rapid precision functional mapping of individuals using multi-echo fMRI. Cell Rep. 33 (12), 108540 https://doi.org/10.1016/j.celrep.2020.108540.

Marinkovic, K., 2004. Spatiotemporal dynamics of word processing in the human cortex. Neuroscientist 10 (2), 142–152. https://doi.org/10.1177/1073858403261018.

Marinkovic, K., Beaton, L.E., Rosen, B.Q., Happer, J.P., Wagner, L.C., 2019. Disruption of frontal lobe neural synchrony during cognitive control by alcohol intoxication. JoVE : JoVE 144, e58839. https://doi.org/10.3791/58839.

Marinkovic, K., Dhond, R.P., Dale, A.M., Glessner, M., Carr, V., Halgren, E., 2003. Spatiotemporal dynamics of modality-specific and supramodal word processing. Neuron 38 (3), 487–497. https://doi.org/10.1016/S0896-6273(03)00197-1.

Marinkovic, K., Rosen, B.Q., Cox, B., Hagler Jr., D.J., 2014. Spatio-temporal processing of words and nonwords: hemispheric laterality and acute alcohol intoxication. Brain Res. 1558, 18–32. https://doi.org/10.1016/j.brainres.2014.02.030.

Marinkovic, K., Rosen, B.Q., Cox, B., Kovacevic, S., 2012. Event-related theta power during lexical-semantic retrieval and decision conflict is modulated by alcohol intoxication: anatomically constrained MEG. Front. Psychol. 3 (APR), 121. https://doi.org/10.3389/fpsyg.2012.00121.

Mash, L.E., Reiter, M.A., Linke, A.C., Townsend, J., Müller, R.A., 2018. Multimodal approaches to functional connectivity in autism spectrum disorders: an integrative perspective. Dev. Neurobiol. 78 (5), 456–473. https://doi.org/10.1002/dneu.22570.

May, K.E., Kana, R.K., 2020. Frontoparietal network in executive functioning in autism spectrum disorder. Autism Res. 13 (10), 1762–1777. https://doi.org/10.1002/aur.2403.

McGregor, K.K., Berns, A.J., Owen, A.J., Michels, S.A., Duff, D., Bahnsen, A.J., Lloyd, M., 2012. Associations between syntax and the lexicon among children with or without

ASD and language impairment. J. Autism Dev. Disord. 42 (1), 35–47. https://doi.org/10.1007/s10803-011-1210-4.
Meltzer, J.A., Negishi, M., Mayes, L.C., Constable, R.T., 2007. Individual differences in EEG theta and alpha dynamics during working memory correlate with fMRI responses across subjects. Clin. Neurophysiol. 118 (11), 2419–2436. https://doi.org/10.1016/j.trsl.2012.08.005.
Moseley, R.L., Mohr, B., Lombardo, M.V., Baron-Cohen, S., Hauk, O., Pulvermüller, F., 2013. Brain and behavioral correlates of action semantic deficits in autism. Front. Hum. Neurosci. 7 (NOV), 1–10. https://doi.org/10.3389/fnhum.2013.00725.
Naigles, L.R., Tek, S., 2017. 'Form is easy, meaning is hard' revisited: (re) characterizing the strengths and weaknesses of language in children with autism spectrum disorder. Wiley Interdisciplinary Rev.: Cognit. Sci. 8 (4), 1–12. https://doi.org/10.1002/wcs.1438.
Olafsson, V., Kundu, P., Wong, E.C., Bandettini, P.A., Liu, T.T., 2015. Enhanced identification of BOLD-like components with multi-echo simultaneous multi-slice (MESMS) fMRI and multi-echo ICA. Neuroimage 112, 43–51. https://doi.org/10.1016/j.neuroimage.2015.02.052.
Oldfield, R.C., 1971. The assessment and analysis of handedness: the edinburgh inventory. In: Neuropsychologia, vol. 9. Pergamon Press.
Oostenveld, R., Fries, P., Maris, E., Schoffelen, J.M., 2011. FieldTrip: open source software for advanced analysis of MEG, EEG, and invasive electrophysiological data. Comput. Intell. Neurosci. https://doi.org/10.1155/2011/156869, 2011.
Padmanabhan, P., Nedumaran, A.M., Mishra, S., Pandarinathan, G., Archunan, G., Gulyás, B., 2017. The advents of hybrid imaging modalities: a new era in neuroimaging applications. Advanced Biosystems 1 (8), 1–17. https://doi.org/10.1002/adbi.201700019.
Posner, M.I., Rothbart, M.K., Sheese, B.E., 2007. The anterior cingulate gyrus and the mechanism of self-regulation. Cognit. Affect Behav. Neurosci. 7 (4), 391–395. https://doi.org/10.3758/CABN.7.4.391.
Pu, Y., Cheyne, D., Sun, Y., Johnson, B.W., 2020. Theta oscillations support the interface between language and memory. Neuroimage 215. https://doi.org/10.1016/j.neuroimage.2020.116782.
Rajan, A., Siegel, S.N., Liu, Y., Bengson, J., Mangun, G.R., Ding, M., 2019. Theta oscillations index frontal decision-making and mediate reciprocal frontal-parietal interactions in willed attention. Cerebr. Cortex 29 (7), 2832–2843. https://doi.org/10.1093/cercor/bhy149.
Reynell, C., Harris, J.J., 2013. The BOLD signal and neurovascular coupling in autism. Dev. Cognitive Neurosci. 6, 72–79. https://doi.org/10.1016/j.dcn.2013.07.003.
Rosen, B.Q., Padovan, N., Marinkovic, K., 2016. Alcohol hits you when it is hard: intoxication, task difficulty, and theta brain oscillations. Alcohol Clin. Exp. Res. 40 (4), 743–752. https://doi.org/10.1111/acer.13014.
Ruff, I., Blumstein, S.E., Myers, E.B., Hutchison, E., 2008. Recruitment of anterior and posterior structures in lexical-semantic processing: an fMRI study comparing implicit and explicit tasks. Brain Lang. 105 (1), 41–49. https://doi.org/10.1016/j.bandl.2008.01.003.
Rutter, M., LeCouteur, A., Lord, C., 2003. Autism Diagnostic Interview-Revised Manual. Western Psychological Services.
Sahyoun, C.P., Belliveau, J.W., Soulières, I., Schwartz, S., Mody, M., 2010. Neuroimaging of the functional and structural networks underlying visuospatial vs. linguistic reasoning in high-functioning autism. Neuropsychologia 48 (1), 86–95. https://doi.org/10.1016/j.neuropsychologia.2009.08.013.
Schaefer, A., Kong, R., Gordon, E.M., Laumann, T.O., Zuo, X.-N., Holmes, A.J., Eickhoff, S.B., Yeo, B.T.T., 2018. Local-global parcellation of the human cerebral cortex from intrinsic functional connectivity MRI. Cerebr. Cortex 28 (9), 3095–3114. https://doi.org/10.1093/cercor/bhx179.
Scheeringa, R., Fries, P., 2019. Cortical layers, rhythms and BOLD signals. Neuroimage 197, 689–698. https://doi.org/10.1016/j.neuroimage.2017.11.002. October 2017.
Scheeringa, R., Petersson, K.M., Oostenveld, R., Norris, D.G., Hagoort, P., Bastiaansen, M.C.M., 2009. Trial-by-trial coupling between EEG and BOLD identifies networks related to alpha and theta EEG power increases during working memory maintenance. Neuroimage 44 (3), 1224–1238. https://doi.org/10.1016/j.neuroimage.2008.08.041.
Semel, E., Wiig, E., Secord, W.A., 2013. Clinical Evaluation of Language Fundamentals. Pearson.
Shen, M.D., Shih, P., Öttl, B., Keehn, B., Leyden, K.M., Gaffrey, M.S., Müller, R.A., 2012. Atypical lexicosemantic function of extrastriate cortex in autism spectrum disorder: evidence from functional and effective connectivity. Neuroimage 62 (3), 1780–1791. https://doi.org/10.1016/j.neuroimage.2012.06.008.
Singh, K.D., Barnes, G.R., Hillebrand, A., Forde, E.M.E., Williams, A.L., 2002. Task-related changes in cortical synchronization are spatially coincident with the hemodynamic response. Neuroimage 16 (1), 103–114. https://doi.org/10.1006/nimg.2001.1050.
Smith, S.M., Jenkinson, M., Woolrich, M.W., Beckmann, C.F., Behrens, T.E.J., Johansen-Berg, H., Bannister, P.R., De Luca, M., Drobnjak, I., Flitney, D.E., Niazy, R.K., Saunders, J., Vickers, J., Zhang, Y., De Stefano, N., Brady, J.M., Matthews, P.M., 2004. Advances in functional and structural MR image analysis and implementation as FSL. Neuroimage 23 (Suppl. 1), S208–S219. https://doi.org/10.1016/j.neuroimage.2004.07.051.
Tsujimoto, T., Shimazu, H., Isomura, Y., 2006. Direct recording of theta oscillations in primate prefrontal and anterior cingulate cortices. J. Neurophysiol. 95 (5), 2987–3000. https://doi.org/10.1152/jn.00730.2005.
Van Heuven, W.J.B., Mandera, P., Keuleers, E., Brysbaert, M., 2014. SUBTLEX-UK: a new and improved word frequency database for British English. Q. J. Exp. Psychol. 67 (6), 1176–1190. https://doi.org/10.1080/17470218.2013.850521.
Wechsler, D., 2009. Wechsler Individual Achievement Test, third ed. Psychological Corporation.
Wechsler, D., 2011. Wechsler Abbreviated Scale of Intelligence, second ed. NCS Pearson.
Winterer, G., Carver, F.W., Musso, F., Mattay, V., Weinberger, D.R., Coppola, R., 2007. Complex relationship between BOLD signal and synchronization/desynchronization of human brain MEG oscillations. Hum. Brain Mapp. 28 (9), 805–816. https://doi.org/10.1002/hbm.20322.
You, Y., Correas, A., Jao Keehn, R.J., Wagner, L.C., Rosen, B.Q., Beaton, L.E., Gao, Y., Brocklehurst, W.T., Fishman, I., Müller, R.-A., Marinkovic, K., 2020. MEG theta during lexico-semantic and executive processing is altered in high-functioning adolescents with autism. Cerebr. Cortex 1–15. https://doi.org/10.1093/cercor/bhaa279.
Zhang, Z., Peng, P., Zhang, D., 2020. Executive function in high-functioning autism spectrum disorder: a meta-analysis of fMRI studies. J. Autism Dev. Disord. 50 (11), 4022–4038. https://doi.org/10.1007/s10803-020-04461-z.